

---

# Consistency regularization and CutMix for semi-supervised semantic segmentation

---

**Geoff French \***

University of East Anglia, Norwich, UK  
g.french@uea.ac.uk

**Timo Aila**

NVIDIA  
taila@nvidia.com

**Samuli Laine**

NVIDIA  
slaine@nvidia.com

**Michal Mackiewicz**

University of East Anglia, Norwich, UK  
m.mackiewicz@uea.ac.uk

**Graham Finlayson**

University of East Anglia, Norwich, UK  
g.finlayson@uea.ac.uk

## Abstract

Consistency regularization describes a class of approaches that have yielded ground breaking results in semi-supervised classification problems. Prior work has established the *cluster assumption* – under which the data distribution consists of uniform class clusters of samples separated by low density regions – as key to its success. We analyse the problem of semantic segmentation and find that the data distribution does not exhibit low density regions separating classes and offer this as an explanation for why semi-supervised segmentation is a challenging problem. We adapt the recently proposed CutMix regularizer for semantic segmentation and find that it is able to overcome this obstacle, leading to a successful application of consistency regularization to semi-supervised semantic segmentation.

## 1 Introduction

Semi-supervised learning offers the tantalising promise of training a machine learning model with limited amounts of labelled training data and large quantities of unlabelled data. These situations often arise in practical computer vision problems where large quantities of images are readily available and generating ground truth labels acts as a bottleneck due to the cost and labour required. Consistency regularization [20] describes a class of semi-supervised learning algorithms used to train deep neural network classifiers that have yielded state-of-the-art semi-supervised classification results, while being conceptually simple and often easy to implement.

Prior work has established the *cluster assumption* [19, 18, 30] as key to the success of consistency regularization based approaches. The cluster assumption holds when a data distribution consists of uniform class clusters that are separated by regions of low sample density. We present a simple toy 2D classification problem in which we confirm the benefit of the clustered data. Subsequently we find that appropriately constrained consistency regularization can operate on data with a continuous distribution (no low density regions).

Semantic segmentation networks can be considered to operate as fully-convolutional patch classifiers that process the patches within an image in a sliding window fashion. We contribute the observation that the  $L^2$  distance between the contents of patches centred on neighbouring pixels within an image varies smoothly and show that low density regions within the distribution do not lie on class boundaries. This leads us to explore strategies for guiding consistency regularization that can operate in these conditions. We contribute a variant of CutMix [31] adapted for semantic segmentation and

---

\*Part of this work was done during an internship at NVIDIA Research

contrast it to standard data augmentation. We find that our adapted CutMix regularizer improves performance in semi-supervised semantic segmentation problems and achieves results competitive with the adversarial approach of Hung *et al.* [12].

Our paper is arranged as follows: in Section 2 we review the literature relevant to our work. We analyse the properties and mechanisms of consistency regularization in Section 3. In Section 4 we analyse semantic segmentation problems and ascertain why semi-supervised segmentation has proved to be challenging in the past and propose two approaches to overcome these difficulties. We describe our experiments and present our results in Section 5. We present our conclusions in Section 6.

## 2 Background

Our work relates to prior art from three areas that we will review here. First we will review the recently proposed MixUp and CutMix regularizers designed for supervised classifiers. After this we will discuss work related to semi-supervised classification with a focus on consistency regularization. Finally we will cover semantic segmentation.

### 2.1 MixUp and CutMix

The MixUp regularizer of Zhang *et al.* [32] improved the performance of supervised classifiers by using interpolated samples during training. Each interpolated training sample with corresponding ground truth results from blending the image pixels and blending the ground truth labels of two randomly chosen samples from the training set.

The recently proposed CutMix regularizer of Yun *et al.* [31] blends pairs of training samples by cutting a rectangular region from the second image and pasting it over the first. Both MixUp and CutMix improve supervised image classification performance, with CutMix outperforming MixUp. MixUp is also able to improve performance on speech and tabular data.

### 2.2 Semi-supervised classification

Consistency regularization describes a class of techniques in which a network is trained to make consistent predictions in response to perturbation of unlabeled samples. They normally combine a standard supervised loss term (e.g. cross-entropy loss) with a consistency loss term. The term consistency regularization was popularized by Oliver *et al.* [20]. They provide an overview and evaluation of semi-supervised learning approaches. We will now discuss several consistency regularization based approaches.

The  $\Pi$ -model of Laine *et al.* [16] passes each unlabeled sample through a classifier twice, using stochastic augmentation, dropout and Gaussian noise to provide perturbation. They minimize the difference between the class probability predictions resulting from the two presentations of each sample. Their temporal model maintains a per-sample moving average of historical predictions and encourages subsequent predictions to be consistent with the average. Similarly Sajjadi *et al.* [25] maintain a history of predictions for each unlabelled sample and encourage consistency between the current and historical predictions.

The mean teacher model of Tarvainen *et al.* [29] encourages consistency between predictions from two neural networks; the student and the teacher. The student is trained using gradient descent. The weights of the teacher are computed using Polyak averaging [22]; they are an exponential moving average of those of the student. French *et al.* [10] adapted the mean teacher approach for domain adaptation.

Miyato *et al.* [19] introduced virtual adversarial training in which perturbation takes the form of adversarial examples. They maximise the change in class prediction by computing the gradient of the prediction change with respect to the input image pixels.

Interpolation consistency training (ICT) by Verma *et al.* [30] and MixMatch by Berthelot *et al.* [3] both combine MixUp [32] with consistency regularization. ICT uses the mean teacher model [29] and applies MixUp to unsupervised samples, blending input images along with teacher class predictions to produce a blended input and target to train the student. MixMatch stochastically augments each

sample multiple times and averages the predictions to produce unsupervised targets. MixUp is applied to the predictions for unsupervised samples and ground truths for supervised samples.

Explanations of the mechanism of consistency regularization are based on the *smoothness* assumption and the *cluster* assumption. The smoothness assumption states that samples close to each other are likely to have the same label. Luo *et al.* [18] propose that this underlies the success of recent semi-supervised learning methods. Miyato *et al.* [19] state that virtual adversarial training smooths the decision function in the neighbourhood of unsupervised samples. The *cluster* assumption – a special case of the smoothness assumption – states that decision surfaces in classification scenarios should lie in low density regions, not crossing high density regions [5]. This mechanism is cited by both Sajjadi *et al.* [24] and Shu *et al.* [26].

### 2.3 Semantic segmentation

Witin the last several years deep neural networks have achieved state of the art results for semantic segmentation tasks. Most approaches employ transfer learning, usually using the convolutional layers of the VGG-16 [27] classification network as a backbone.

Long *et al.* introduced the fully convolutional network (FCN) [17] that attached a convolutional 21-way classifier to a VGG-16 [27] backbone, demonstrating the effectiveness of deep neural networks for semantic segmentation. Chen *et al.* used dilated/atrous convolutions [6] in the later layers of VGG-16, increasing the spatial resolution of their predictions while maintaining their receptive fields. The term *fully convolutional network* is now often used to describe networks that use only convolutional layers, therefore producing predictions spaced on a regular grid.

More recent approaches use encoder-decoder networks in which the structure of the decoder mirrors that of the encoder – often a pre-trained classification network – in reverse order. The decoder uses upsampling to increase resolution and skip connections to draw data from layers in the encoder that have the same spatial resolution, improving the ability of the network to accurately segment fine details. Badrinarayanan *et al.* [2] use a VGG-16 based encoder and carry pooling indices from max-pooling layers in the encoder to unpooling layers in the decoder. U-nets [23] use transposed convolution layers to increase resolution and its skip connections carry complete feature maps. U-Nets have become popular among practitioners.

A variety of approaches for semi-supervised semantic segmentation have been proposed. Kalluri *et al.* [14] combined semi-supervised learning and unsupervised domain adaptation. Stekovic *et al.* [28] enforced geometric constraints between multiple views of a 3D scene. Hung *et al.* [12] employed adversarial learning, using a discriminator network that distinguishes real from predicted segmentation maps to guide learning.

## 3 Consistency regularization

In this section we will formally define consistency regularization and explore its properties.

### 3.1 Definition and mechanism

Consistency regularization adds a consistency loss term  $L_{cons}$  to the loss that is minimized during training [20].  $L_{cons}$  measures the distance  $d(\cdot, \cdot)$  between the predictions resulting from applying a neural network  $f_\theta$  parameterized by  $\theta$  to an unsupervised sample  $x$  and a perturbed version of the same sample  $\hat{x}$ :

$$L_{cons} = d(f_\theta(x), f_\theta(\hat{x}))$$

The perturbation used to generate  $\hat{x}$  given  $x$  depends on the variant of consistency regularization used [19, 16]. A variety of distance measures  $d(\cdot, \cdot)$  have been used, e.g. squared distance [16] or cross-entropy [19].

Athiwaratkun *et al.* [1] observed that in the case of a simplified version of the  $\pi$ -model[16] in which perturbation consists of additive Gaussian noise  $\hat{x} = x + h, h \sim \mathcal{N}(0, I)$ , the consistency loss term  $L_{cons}$  is an estimate of the square of the Frobenius norm of the Jacobian  $J_{f_\theta}(x)$  of the networks outputs with respect to its inputs:

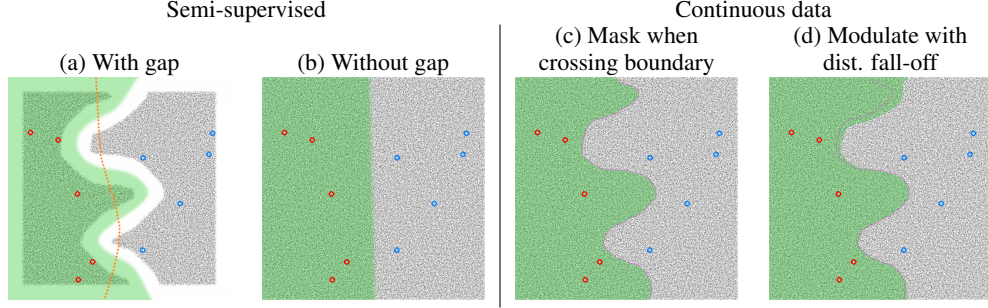


Figure 1: 2D semi-supervised classification experiments. Blue and red circles indicate supervised samples from class 0 and 1 respectively. The field of small black dots indicate unsupervised samples. The decision function is visualised by rendering the probability of class 1 in green; the soft gradation represents the gradual change in predicted class probability. (a) and (b) illustrate semi-supervised learning with and without a gap. The dotted orange line in (a) shows the decision boundary expected with plain supervised learning. (c) and (d) use continuous data. In (c) the consistency loss is masked to 0 when perturbation places  $x$  and  $\hat{x}$  on difference sides of the decision boundary. In (d) the consistency loss is modulated by falloff function that tends from 1 to 0 as the difference in distance to the decision boundary increases.

$$L_{cons} \approx \|J_{f_\theta}(x)\|_F^2$$

### 3.2 Consistency regularization for clustered data

When using isotropic perturbation (e.g. Gaussian noise), minimizing the magnitude of  $J_{f_\theta}$  will smooth the decision function in the vicinity of unsupervised samples as stated in [19], encouraging the network to move the decision boundary – and its surrounding region of high gradient – into regions of low sample density.

We demonstrate this using a simple classification problem in which samples are 2D  $x, y$  points. We use the mean teacher [29] and Gaussian noise for sample perturbation. The baseline decision boundary learned using 10 supervised training samples is shown as a dotted orange line in Figure 1 (a). Applying consistency regularization results in the green decision boundary. If we remove gap that separates the two regions consistency regularization is unable to place the decision boundary in a low density region, so it smooths and straightens it as seen in Figure 1 (b).

### 3.3 Constrained consistency regularization for continuous data

Stochastic data augmentation can be used to provide semantically preserving perturbation [25, 16, 10] that constrains consistency regularization to encourage smoothness *only* in the directions of perturbation. This mechanism allows  $L_{cons}$  to be minimized by orienting the decision boundaries to lie parallel to the directions of perturbation, in addition to settling in low density regions. This could in principal permit its use in situations where there are no low density regions between classes.

We designed two 2D toy experiments to test constrained consistency regularization. In Figure 1 (c) we masked to 0 the consistency loss  $L_{cons}$  for any sample  $x$  and perturbed  $\hat{x}$  where  $x$  and  $\hat{x}$  lie on different sides of the decision boundary. The learned green decision boundary co-incides with the magenta ground truth boundary almost perfectly.

In Figure 1 (d) we compute the distances  $b(x)$  and  $b(\hat{x})$  from  $x$  and  $\hat{x}$  to the decision boundary and weight  $L_{cons}$  by a Gaussian fall-off function  $e^{-\sigma(b(x)-b(\hat{x}))^2}$ . This constraints consistency loss to perturbations that preserve distance to the decision boundary, mimicing an augmentation-based scenario in which we enforce consistency in semantically preserving directions.

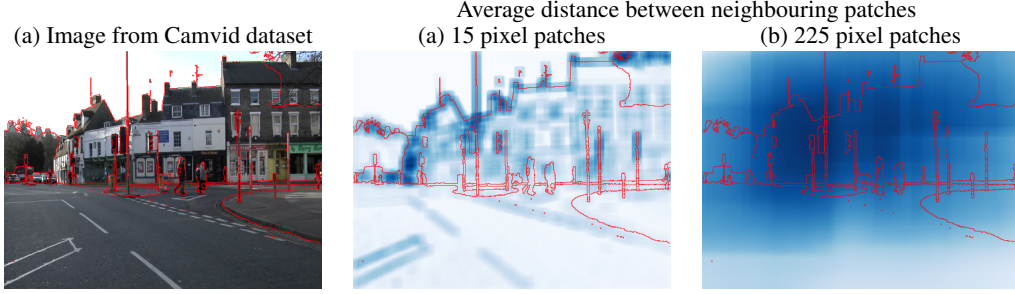


Figure 2: An illustration showing that low density regions do not lie along all class boundaries. (a) An image from Camvid dataset along with average  $L^2$  distance from a patch to its four immediate neighbours using patch sizes of (b) 15 pixels and (c) 225 pixels. Dark blue indicates large inter-patch distance and therefore a low density region, white indicates a distance of 0. The red lines indicate segmentation ground truth boundaries.

## 4 Consistency regularization for semantic segmentation

Consistency regularization would appear to be a promising avenue as semantic segmentation can be viewed as pixel classification. There are however few reports of success [21] in the literature. We explain this with an observation of the nature of semantic segmentation that indicates that there are no low density regions between classes. Subsequently we explain two approaches for driving consistency regularization that have the potential to work when the cluster assumption does not hold.

### 4.1 No low density regions between classes

As has been established the presence of low density regions separating class regions are very effective at guiding consistency regularization. Our explanation for its infrequent of success in semantic segmentation problems rests on the fact that low density regions do not align with class boundaries.

Modern segmentation networks are implemented as fully convolutional networks that output pixel-wise classification. In effect they operate as classifiers that are applied in a sliding window fashion, re-using shared computation among overlapping windows. The input corresponding to each pixel is a patch centred on that pixel, whose dimensions are determined by the receptive field of the network.

Low density regions separating classes in semantic segmentation problems would present as locally larger than average differences (measured using  $L^2$  distance) between the pixel content of patches whose central pixels are immediate neighbours that lie on either side of a class boundary.

The squared distance between all immediately horizontally neighbouring patches  $D_x$  can be computed by applying a box filter to the square of the horizontal gradient image (square difference between horizontally neighbouring pixels) where the filter width (and height) is equal to the patch width. The same can be done for the distance between vertically neighbouring patches  $D_y$ .

$$D_x = \sqrt{B * (\nabla I)_x^2}$$

where  $B$  is a box filter kernel

Uniform filters act as low-pass filters, suppressing the fine details found in the high frequency components of the image. This can be seen in Figure 2(b) and (c) that show the average distance between a patch and its 4 immediate neighbours with patch widths of 15 and 225 pixels respectively. Darker regions correspond to larger distances between neighbours and indicate low density. In Figure 2(b) they coincide only with class boundaries that lie along strong edges in the image (e.g. the border between light coloured sky and darker buildings). A patch width of only 15 pixels however provides insufficient context for accurate segmentation. Increasing the patch width to 225 pixels (a more reasonable receptive field) results in the complete loss of fine detail and of the low density regions that could guide consistency regularization.

## 4.2 Consistency regularization without the cluster assumption

In light of the continuous distribution experiments in Section 3.3, the findings above motivate us to explore strategies for driving consistency regularization that do not depend on the cluster assumption. To this end we evaluate augmentation based perturbation and CutMix.

### 4.2.1 Augmentation based perturbation

As discussed in Section 3.3, applying stochastic augmentation results in semantically preserving perturbations that lie on the image manifold [1]. We use the augmentation scheme here as we do in our other experiments (see Section 5.2).

An unlabeled sample is augmented twice using different augmentation parameters; one is passed through the teacher network, the other through the student. The networks predict pre-softmax class logits  $l_t(x)$  and  $l_s(x)$  respectively. If the matrix  $m_t$  describes the affine transformation applied by the teacher path augmentation and  $m_s$  the student path augmentation, we compute  $m_{st} = m_t m_s^{-1}$  and use it to transform the student path logits  $l_s(x)$  into the same co-ordinate frame as those of the teacher, resulting in logits  $l_{st}(x)$ . From these aligned predictions we compute class probabilities using softmax and compute consistency loss using squared difference [16]. We mask the per-pixel consistency loss so that it is only applied to pixels that are not transformed outside the bounds of the image by the affine transformations used in either path. A similar approach is used in [13]. We used a consistency loss weight of 0.3.

### 4.2.2 CutMix for segmentation

The CutMix algorithm was originally designed for classification. It mixes samples by cutting and pasting a rectangular region from one sample into another. We adapted it for semantic segmentation by generating  $N = 32$  rectangular mixing regions with random sizes and positions. The total area of the regions will be approximately half the area of the image of dimensions  $W, H$ . The dimensions  $w_i, h_i$  of each region  $i$  is determined by a scale  $s$  and an aspect ratio  $r$ :

$$\begin{aligned} s &\sim e^{\mathcal{U}(-\ln 2, \ln 2)} \sqrt{\frac{WH}{2N}} \\ r &\sim e^{\mathcal{N}(0, 1)} \\ [w_i, h_i] &= [s\sqrt{r}, \frac{s}{\sqrt{r}}] \end{aligned}$$

Each region is cropped from a random position  $u_i, v_i$  in image  $x_b$  and pasted into a random position  $p_i, q_i$  in image  $x_a$ . The top left corners are both drawn such that they reside within the bounds of the image:

$$[u_i, v_i] \sim [\mathcal{U}(0, 1)(W - w_i), \mathcal{U}(0, 1)(H - h_i)]$$

We denote the mixing of two images  $x_a$  and  $x_b$  with the sequence of cuts  $K = \{k_1 \dots k_N\}$  where  $k_i = [w_i, h_i, p_i, q_i, u_i, v_i]$  as  $cutmix(x_a, x_b, K)$ .

The unlabeled samples are augmented using the scheme described in Section 5.2. Two unlabelled samples  $x_a$  and  $x_b$  are selected and passed through the teacher network resulting in predicted class probabilities  $p_t(x_a)$  and  $p_t(x_b)$ . The augmented images and teacher predictions are mixed using CutMix;  $x_m = cutmix(x_a, x_b, K)$  and  $p_{mt}(x_a, x_b) = cutmix(p_t(x_a), p_t(x_b), K)$ . The mixed image  $x_m$  is passed to the student network resulting in predictions  $p_s(x_m)$ . The consistency loss term is the squared difference between the students predicted probabilities from the mixed image  $p_s(x_m)$  and the mixed teacher predicted probabilities  $p_{mt}(x_a, x_b)$ . We used a consistency loss weight of 10. CutMix is illustrated in Figure 3 and in the supplementary material.

## 5 Experiments

In this section we will describe our experiments. We will discuss the network architecture, training procedure and present our results. Our implementation uses the PyTorch [7] framework.<sup>2</sup>

<sup>2</sup>Our code is available at [TBA](#)

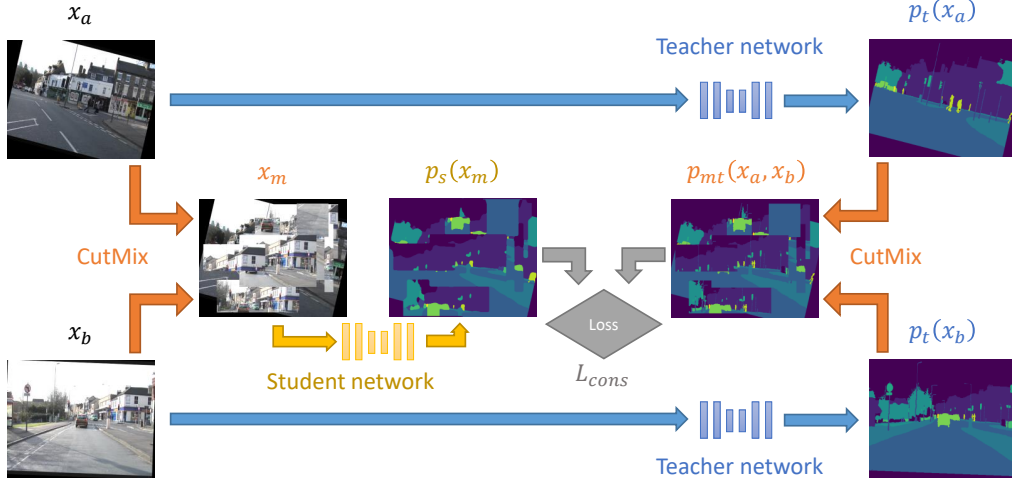


Figure 3: Illustration of unsupervised CutMix loss for semi-supervised semantic segmentation

### 5.1 Network architecture

Our network is a U-Net [23] with an ImageNet pre-trained ResNet-50 [11] based encoder. The decoder consists of alternating  $3 \times 3$  convolutions and strided  $4 \times 4$  transposed convolutions. We describe it in more detail in the supplementary material.

### 5.2 Training procedure

Our data augmentation consists of an affine transformation composed of horizontal flips, translation in the range  $[-4, 4]$  pixels, uniform scaling in the range  $[0.8, 1.25]$  and rotation in the range  $[-15^\circ, 15^\circ]$ . We also modify the brightness and contrast by adding a value  $b \sim \mathcal{N}(0, 0.1)$  and scaling by a factor  $c \sim e^{\mathcal{N}(0, \ln(1.1))}$ .

French *et al.* [10] apply confidence thresholding, in which they mask consistency loss for samples whose confidence as predicted by the teacher network is below a threshold of 0.968. In the context of segmentation, we found that this masks pixels close to class boundaries as they usually have a low confidence. These regions are often large enough to encompass small objects, preventing learning and degrading performance. Instead we modulate the consistency loss with the proportion of pixels whose confidence is above the threshold. This values grows throughout training, taking the place of the sigmoidal ramp-up used in [16, 29].

The CamVid [4] and Cityscapes [8] training sets consist of 367 and 2975 images respectively. We chose 10 different subsets – 30 images for CamVid and 100 images for Cityscapes – for supervised learning in our baseline and semi-supervised experiments. All training images were used for computing consistency loss and within our fully supervised experiments.

We tuned our approach and selected hyper-parameters using the CamVid dataset due to its small size and fast run-time, after which we applied the same hyper-parameters to Cityscapes. We did not run the augmentation based perturbation experiments on the Cityscapes dataset due to the long run-time involved.

### 5.3 Results

Our results on the CamVid dataset can be seen in Figure 4 and Table 1. Data augmentation driven consistency regularization results in no measurable improvement in the mean IoU score, although it improves the score in the building, road, pavement and car classes. The use of CutMix provides a clear performance benefit, clearing half the mean IoU difference between the baseline and fully supervised experiments. It provides little improvement on the building, tree and fence classes and slightly reduces performance on the pole class.

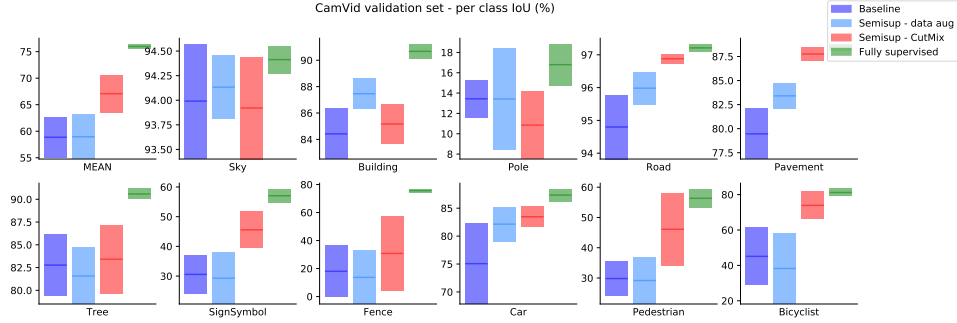


Figure 4: Semi-supervised segmentation on CamVid dataset

Our results on the Cityscapes dataset can be seen in Table 2. Here, CutMix is able to clear approximately one third of the difference between the baseline and fully supervised performance. Our results are slightly ahead of those of Hung *et al.* [12] when using  $\frac{1}{8}$  of the training set for supervised learning, but fall slightly behind when using  $\frac{1}{4}$  or  $\frac{1}{2}$ .

## 5.4 Discussion

We hypothesize that CutMix encourages the network to learn to recognise objects in spite of the fact that they can be obscured [9], forcing the network to learn more robust representations. The use of other mask shapes besides rectangles are a direction for future work.

	Mean IoU
Baseline	58.86% $\pm 3.84$
Data augmentation	58.96% $\pm 4.20$
CutMix	67.08% $\pm 3.56$
Fully supervised	75.97% $\pm 0.47$

Table 1: Performance on CamVid validation set. Our results are mean intersection-over-union (mIoU) presented as *mean*  $\pm$  *stdev*. Per-class results can be found in the supplementary material.

# sup. samples	100	372 ( $\frac{1}{8}$ )	744 ( $\frac{1}{4}$ )	1488 ( $\frac{1}{2}$ )	Full
Adversarial by Hung <i>et al.</i> [12]					
Baseline	—	55.5%	59.9%	64.1%	65.3%
Semi-supervised	—	58.8%	62.3%	65.7%	—
Improvement	—	3.5%	2.4%	1.6%	—
Our results					
Baseline	48.90% $\pm 0.87$	59.41% $\pm 0.24$	63.63% $\pm 0.04$	66.51% $\pm 0.14$	68.47% $\pm 0.64$
CutMix	55.39% $\pm 2.19$	63.41% $\pm 0.28$	65.25% $\pm 0.14$	67.75% $\pm 0.14$	—
Improvement	6.49%	4.01%	1.62%	1.24%	—

Table 2: Performance on cityscapes validation set. The results for 100 samples and fully supervised are computed from 10 runs while our results for 374, 744 and 1488 samples are computed from 2 runs, limited due to time constraints. Per-class results can be found in the supplementary material.

## 6 Conclusions

We have presented an effective and reliable approach for semi-supervised semantic segmentation based on the recently proposed CutMix regularizer [31] and consistency regularization. Semi-supervised segmentation is a challenging problem due to the fact that the data distribution does not exhibit low density regions between classes necessary for the cluster assumption to hold. The cluster assumption has been noted by other researchers to underpin the success of many semi-supervised classification algorithms presented in prior work. Our results demonstrate that consistency



regularization – a class of simple and effective semi-supervised learning algorithms – can function in these challenging conditions. We believe that problems where the cluster assumption does not hold are a valuable direction for future research.

## Acknowledgments

We would like to thank the following people and organizations:

Janne Hellsten at NVIDIA for his help in running experiments on their infrastructure during the final hours of the writing of this paper; the University of East Anglia High Performance Computing Cluster for the use of their computing resources; and NVIDIA for their generous donation of a Titan X GPU.

## References

- [1] Ben Athiwaratkun, Marc Finzi, Pavel Izmailov, and Andrew Gordon Wilson. There are many consistent explanations of unlabeled data: Why you should average. 2019.
- [2] Vijay Badrinarayanan, Alex Kendall, and Roberto Cipolla. Segnet: A deep convolutional encoder-decoder architecture for image segmentation. *CoRR*, abs/1511.00561, 2015.
- [3] David Berthelot, Nicholas Carlini, Ian Goodfellow, Nicolas Papernot, Avital Oliver, and Colin Raffel. Mixmatch: A holistic approach to semi-supervised learning. *arXiv preprint arXiv:1905.02249*, 2019.
- [4] Gabriel J. Brostow, Julien Fauqueur, and Roberto Cipolla. Semantic object classes in video: A high-definition ground truth database. *Pattern Recognition Letters*, xx(x):xx–xx, 2008.
- [5] Olivier Chapelle and Alexander Zien. Semi-supervised classification by low density separation. In *AISTATS*, volume 2005, pages 57–64. Citeseer, 2005.
- [6] Liang-Chieh Chen, George Papandreou, Iasonas Kokkinos, Kevin Murphy, and Alan L Yuille. Semantic image segmentation with deep convolutional nets and fully connected crfs. *arXiv preprint arXiv:1412.7062*, 2014.
- [7] S. Chintala et al. Pytorch.
- [8] Marius Cordts, Mohamed Omran, Sebastian Ramos, Timo Rehfeld, Markus Enzweiler, Rodrigo Benenson, Uwe Franke, Stefan Roth, and Bernt Schiele. The cityscapes dataset for semantic urban scene understanding. In *Proc. of the IEEE Conference on Computer Vision and Pattern Recognition (CVPR)*, 2016.
- [9] Terrance DeVries and Graham W Taylor. Improved regularization of convolutional neural networks with cutout. *arXiv preprint arXiv:1708.04552*, 2017.
- [10] Geoff French, Michal Mackiewicz, and Mark Fisher. Self-ensembling for visual domain adaptation. In *International Conference on Learning Representations*, 2018.
- [11] Kaiming He, Xiangyu Zhang, Shaoqing Ren, and Jian Sun. Deep residual learning for image recognition. In *Proceedings of the IEEE Conference on Computer Vision and Pattern Recognition*, pages 770–778, 2016.
- [12] Wei-Chih Hung, Yi-Hsuan Tsai, Yan-Ting Liou, Yen-Yu Lin, and Ming-Hsuan Yang. Adversarial learning for semi-supervised semantic segmentation. *arXiv preprint arXiv:1802.07934*, 2018.
- [13] Xu Ji, João F. Henriques, and Andrea Vedaldi. Invariant information distillation for unsupervised image segmentation and clustering. *CoRR*, abs/1807.06653, 2018.
- [14] Tarun Kalluri, Girish Varma, Manmohan Chandraker, and CV Jawahar. Universal semi-supervised semantic segmentation. *arXiv preprint arXiv:1811.10323*, 2018.
- [15] Diederik Kingma and Jimmy Ba. Adam: A method for stochastic optimization. In *ICLR*, 2015.
- [16] Samuli Laine and Timo Aila. Temporal ensembling for semi-supervised learning. In *International Conference on Learning Representations*, 2017.
- [17] Jonathan Long, Evan Shelhamer, and Trevor Darrell. Fully convolutional networks for semantic segmentation. In *Proceedings of the IEEE Conference on Computer Vision and Pattern Recognition*, pages 3431–3440, 2015.
- [18] Yucen Luo, Jun Zhu, Mengxi Li, Yong Ren, and Bo Zhang. Smooth neighbors on teacher graphs for semi-supervised learning. In *Proceedings of the IEEE Conference on Computer Vision and Pattern Recognition*, pages 8896–8905, 2018.
- [19] Takeru Miyato, Schi-ichi Maeda, Masanori Koyama, and Shin Ishii. Virtual adversarial training: a regularization method for supervised and semi-supervised learning. *arXiv preprint arXiv:1704.03976*, 2017.

- [20] Avital Oliver, Augustus Odena, Colin Raffel, Ekin D. Cubuk, and Ian J. Goodfellow. Realistic evaluation of semi-supervised learning algorithms. In *International Conference on Learning Representations*, 2018.
- [21] Christian S Perone and Julien Cohen-Adad. Deep semi-supervised segmentation with weight-averaged consistency targets. In *Deep Learning in Medical Image Analysis and Multimodal Learning for Clinical Decision Support*, pages 12–19. Springer, 2018.
- [22] Boris T Polyak and Anatoli B Juditsky. Acceleration of stochastic approximation by averaging. *SIAM Journal on Control and Optimization*, 30(4):838–855, 1992.
- [23] Olaf Ronneberger, Philipp Fischer, and Thomas Brox. U-net: Convolutional networks for biomedical image segmentation. In *International Conference on Medical Image Computing and Computer-Assisted Intervention*, pages 234–241. Springer, 2015.
- [24] Mehdi Sajjadi, Mehran Javanmardi, and Tolga Tasdizen. Mutual exclusivity loss for semi-supervised deep learning. In *23rd IEEE International Conference on Image Processing, ICIP 2016*. IEEE Computer Society, 2016.
- [25] Mehdi Sajjadi, Mehran Javanmardi, and Tolga Tasdizen. Regularization with stochastic transformations and perturbations for deep semi-supervised learning. In *Advances in Neural Information Processing Systems*, pages 1163–1171, 2016.
- [26] Rui Shu, Hung Bui, Hirokazu Narui, and Stefano Ermon. A DIRT-t approach to unsupervised domain adaptation. In *International Conference on Learning Representations*, 2018.
- [27] K. Simonyan and A. Zisserman. Very deep convolutional networks for large-scale image recognition. *CoRR*, abs/1409.1556, 2014.
- [28] Sinisa Stekovic, Friedrich Fraundorfer, and Vincent Lepetit. S4-net: Geometry-consistent semi-supervised semantic segmentation. *arXiv preprint arXiv:1812.10717*, 2018.
- [29] Antti Tarvainen and Harri Valpola. Mean teachers are better role models: Weight-averaged consistency targets improve semi-supervised deep learning results. In *Advances in neural information processing systems*, pages 1195–1204, 2017.
- [30] Vikas Verma, Alex Lamb, Juho Kannala, Yoshua Bengio, and David Lopez-Paz. Interpolation consistency training for semi-supervised learning. *arXiv preprint arXiv:1903.03825*, 2019.
- [31] Sangdoo Yun, Dongyoon Han, Seong Joon Oh, Sanghyuk Chun, Junsuk Choe, and Youngjoon Yoo. Cutmix: Regularization strategy to train strong classifiers with localizable features. *arXiv preprint arXiv:1905.04899*, 2019.
- [32] Hongyi Zhang, Moustapha Cisse, Yann N. Dauphin, and David Lopez-Paz. mixup: Beyond empirical risk minimization. In *International Conference on Learning Representations*, 2018.

## A Supplementary material: 2D toy experiments

The neural networks used in our 2D toy experiments are simple classifiers in which samples are 2D  $x, y$  points ranging from -1 to 1. Our networks are multi-layer perceptrons consisting of 3 hidden layers of 512 units, each followed by a ReLu non-linearity. The final layer is a 2-unit classification layer. We use the mean teacher [29] semi-supervised learning algorithm with binary cross-entropy as the consistency loss function, an consistency loss weight of 10, confidence thresholding [?] with a threshold of 0.97. The continuous distribution experiment that uses the distance from the decision boundary to drive a Gaussian fall-off computes consistency loss using squared error applied to the pre-softmax classification logits, rather than the class probabilities. The distances  $b(x)$  and  $b(\hat{x})$  from  $x$  and  $\hat{x}$  to the decision boundary are computed using the distance transform.

## B Supplementary material: semantic segmentation experiments

### B.1 Network architecture

Our network is shown in Figure 5 and Table 3.

### B.2 An example of CutMix

In Figure 6 we present an illustration of the process of CutMix for segmentation.

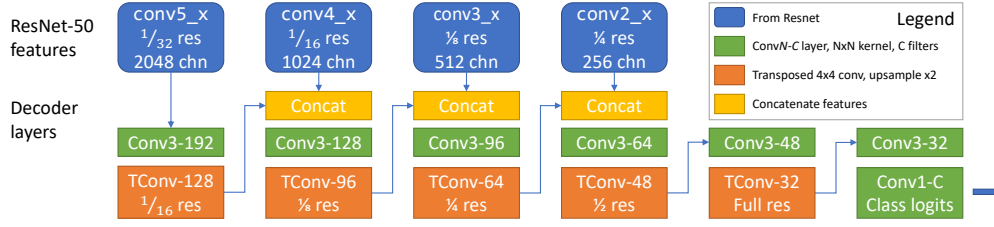


Figure 5: ResNet-50 based U-Net decoder architecture.

Description	Resolution $\times$ channels
ResNet-50 layer conv5_x $\frac{1}{32}$ res, 2048 chn	$\frac{1}{32} \times 2048$
Conv $3 \times 3 \times 192$	$\frac{1}{32} \times 192$
TransposeConv $4 \times 4 \times 128$	$\frac{1}{16} \times 128$
Concat with ResNet-50 layer conv4_x $\frac{1}{16}$ res, 1024 chn	$\frac{1}{16} \times 1152$
Conv $3 \times 3 \times 128$	$\frac{1}{16} \times 128$
TransposeConv $4 \times 4 \times 96$	$\frac{1}{8} \times 96$
Concat with ResNet-50 layer conv3_x $\frac{1}{8}$ res, 512 chn	$\frac{1}{8} \times 608$
Conv $3 \times 3 \times 96$	$\frac{1}{8} \times 96$
TransposeConv $4 \times 4 \times 64$	$\frac{1}{4} \times 64$
Concat with ResNet-50 layer conv2_x $\frac{1}{4}$ res, 256 chn	$\frac{1}{4} \times 320$
Conv $3 \times 3 \times 64$	$\frac{1}{4} \times 64$
TransposeConv $4 \times 4 \times 48$	$\frac{1}{2} \times 48$
Conv $3 \times 3 \times 48$	$\frac{1}{2} \times 48$
TransposeConv $4 \times 4 \times 32$	$1 \times 32$
Conv $3 \times 3 \times 32$	$1 \times 32$
Conv $1 \times 1 \times C$	$1 \times C$

Table 3: ResNet-50 based U-Net decoder.  $C$  is the number of target classes.

### B.3 Training details

In keeping with [17] we use a batch size of 1. We freeze the batch normalization layers within the ResNet encoder, using the pre-trained running mean and variance rather than computing per-batch mean and variance during training. We use the Adam [15] optimization algorithm with a learning rate of  $1 \times 10^{-4}$ . As per the mean teacher algorithm [29], after each iteration the weights  $w_t$  of the teacher network are updated to be the exponential moving average of the weights  $w_s$  of the student:  $w_t = \alpha_t w_t + (1 - \alpha_t) w_s$ , where  $\alpha_t = 0.99$ .

The augmentation based perturbation experiments performed on the CamVid dataset were trained for 150 epochs. The CutMix experiments were trained for 200.

The Cityscapes images were downsampled to half resolution ( $1024 \times 512$ ) prior to use, as in [12]. When using Cityscapes we trained for 100,000 iterations using a batch size of 1.

We tuned our approach and selected hyper-parameters using the CamVid dataset due to its small size and fast run-time, after which we applied the same hyper-parameters to Cityscapes. We did not run the augmentation based perturbation experiments on the Cityscapes dataset due to the long run-time involved.

### B.4 Detailed performance tables

The detailed per-class performance of data augmentation driven consistency regularization and CutMix on the CamVid dataset is presented in Table 4. Our details results on the Cityscapes dataset are presented in Table 5 and visualised in Figure 7.

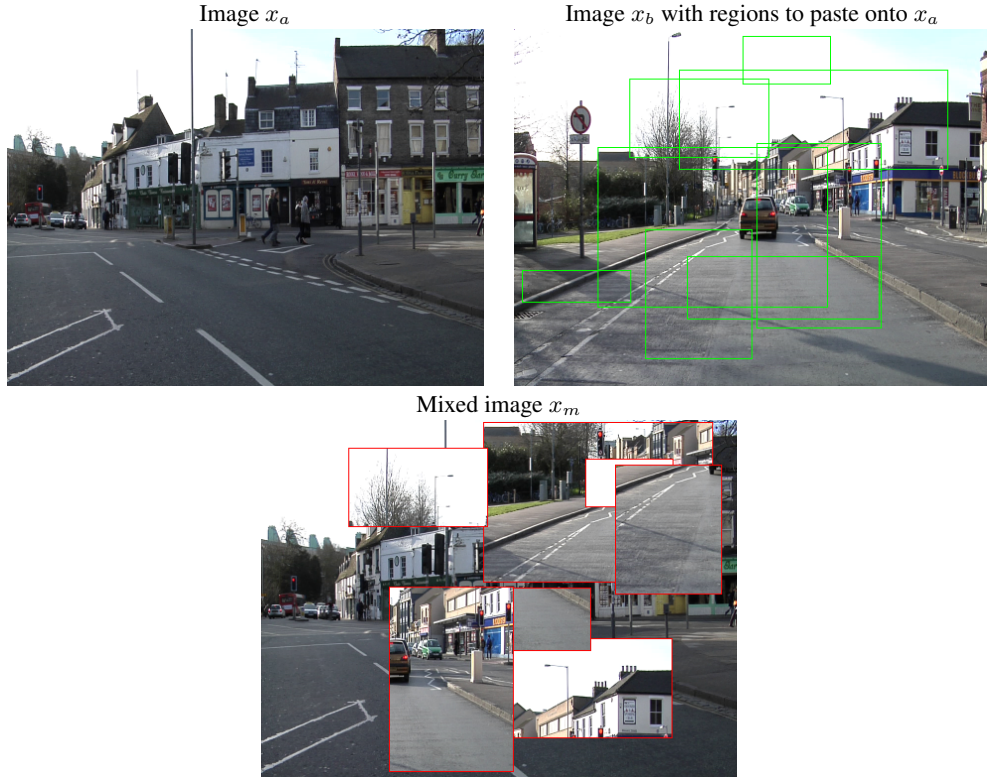


Figure 6: Example of the process of CutMix for segmentation

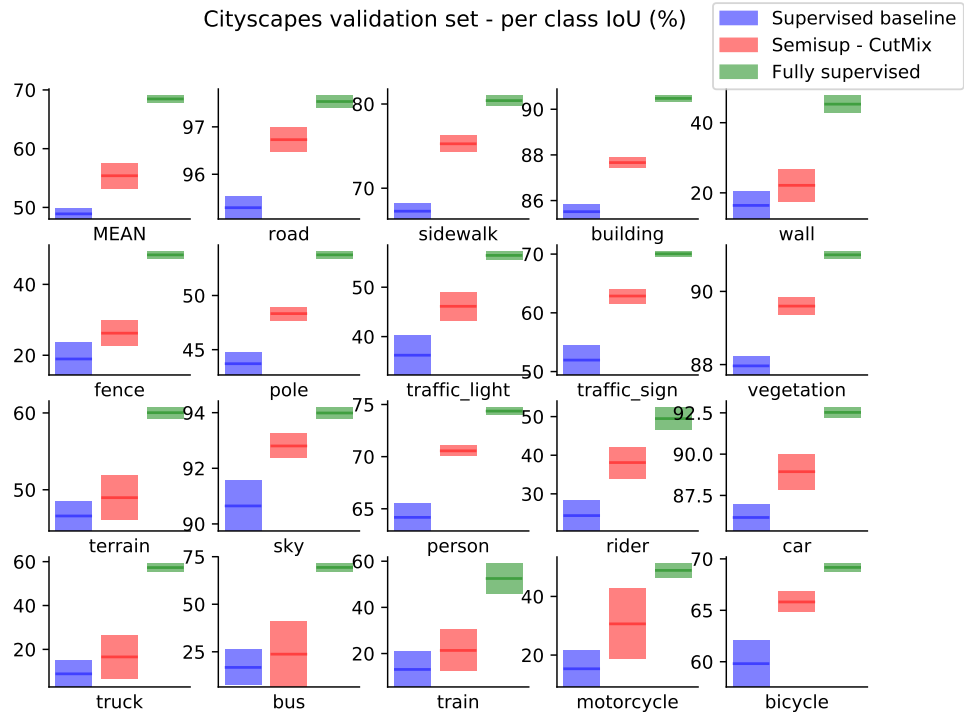


Figure 7: Visualisation of semi-supervised segmentation on Cityscapes dataset

	MEAN IoU	Sky	Building	Pole
Baseline	58.86% $\pm$ 3.84	93.99% $\pm$ 0.58	84.42% $\pm$ 1.91	13.44% $\pm$ 1.83
Data augmentation	58.96% $\pm$ 4.20	94.13% $\pm$ 0.32	87.46% $\pm$ 1.14	13.42% $\pm$ 5.01
CutMix	67.08% $\pm$ 3.56	93.92% $\pm$ 0.52	85.17% $\pm$ 1.50	10.85% $\pm$ 3.34
Fully supervised	75.97% $\pm$ 0.47	94.41% $\pm$ 0.14	90.67% $\pm$ 0.56	16.79% $\pm$ 2.04
	Road	Pavement	Tree	SignSymbol
Baseline	94.80% $\pm$ 0.98	79.46% $\pm$ 2.62	82.77% $\pm$ 3.39	30.57% $\pm$ 6.53
Data augmentation	95.98% $\pm$ 0.50	83.41% $\pm$ 1.31	81.58% $\pm$ 3.07	29.29% $\pm$ 8.69
CutMix	96.88% $\pm$ 0.15	87.76% $\pm$ 0.68	83.42% $\pm$ 3.76	45.56% $\pm$ 6.12
Fully supervised	97.21% $\pm$ 0.12	88.44% $\pm$ 0.36	90.58% $\pm$ 0.55	57.04% $\pm$ 2.29
	Fence	Car	Pedestrian	Bicyclist
Baseline	18.02% $\pm$ 18.22	75.07% $\pm$ 7.22	29.82% $\pm$ 5.64	45.10% $\pm$ 16.32
Data augmentation	13.71% $\pm$ 19.02	82.14% $\pm$ 3.10	29.16% $\pm$ 7.75	38.23% $\pm$ 20.05
CutMix	30.80% $\pm$ 26.50	83.47% $\pm$ 1.85	46.10% $\pm$ 11.92	73.92% $\pm$ 7.82
Fully supervised	75.66% $\pm$ 1.20	87.34% $\pm$ 1.10	56.34% $\pm$ 3.09	81.20% $\pm$ 2.00

Table 4: Per-class performance on CamVid dataset

	MEAN IoU	Road	Sidewalk	Building
Baseline	48.90% $\pm$ 0.87	95.30% $\pm$ 0.24	67.27% $\pm$ 0.92	85.51% $\pm$ 0.32
CutMix	55.39% $\pm$ 2.19	96.73% $\pm$ 0.26	75.27% $\pm$ 0.98	87.66% $\pm$ 0.23
Fully supervised	68.47% $\pm$ 0.64	97.53% $\pm$ 0.13	80.41% $\pm$ 0.64	90.48% $\pm$ 0.14
	Wall	Fence	Pole	Traffic light
Baseline	16.42% $\pm$ 3.87	18.95% $\pm$ 4.52	43.70% $\pm$ 1.04	36.23% $\pm$ 4.00
CutMix	22.14% $\pm$ 4.61	26.23% $\pm$ 3.54	48.33% $\pm$ 0.64	46.13% $\pm$ 2.92
Fully supervised	45.29% $\pm$ 2.56	48.32% $\pm$ 1.04	53.75% $\pm$ 0.34	56.44% $\pm$ 0.86
	Traffic sign	Vegetation	Terrain	Sky
Baseline	51.95% $\pm$ 2.53	87.96% $\pm$ 0.25	46.59% $\pm$ 1.95	90.65% $\pm$ 0.90
CutMix	62.86% $\pm$ 1.27	89.60% $\pm$ 0.24	48.97% $\pm$ 2.88	92.80% $\pm$ 0.44
Fully supervised	70.05% $\pm$ 0.45	91.00% $\pm$ 0.10	60.03% $\pm$ 0.72	93.99% $\pm$ 0.21
	Person	Rider	Car	Truck
Baseline	64.18% $\pm$ 1.30	24.37% $\pm$ 3.98	86.17% $\pm$ 0.82	8.85% $\pm$ 5.98
CutMix	70.56% $\pm$ 0.51	38.10% $\pm$ 4.12	88.94% $\pm$ 1.09	16.56% $\pm$ 10.01
Fully supervised	74.37% $\pm$ 0.38	49.49% $\pm$ 2.96	92.53% $\pm$ 0.32	57.31% $\pm$ 2.01
	Bus	Train	Motorcycle	Bicycle
Baseline	16.79% $\pm$ 9.41	13.10% $\pm$ 7.58	15.32% $\pm$ 6.20	59.81% $\pm$ 2.27
CutMix	23.75% $\pm$ 17.24	21.34% $\pm$ 8.96	30.64% $\pm$ 12.02	65.81% $\pm$ 1.00
Fully supervised	69.36% $\pm$ 2.25	52.51% $\pm$ 6.65	48.88% $\pm$ 2.47	69.17% $\pm$ 0.41

Table 5: Per-class performance on Cityscapes dataset